Available online at www.sciencedirect.com
ScienceDirect
Transportation Research Part C 16 (2008) 116–136
TRANSPORTATION RESEARCH PART C
www.elsevier.com/locate/trc

Investigation of temporal freeway traffic patterns in reconstructed state spaces

Lawrence W. Lan [a,b,1], Jiuh-Biing Sheu [b,2], Yi-San Huang [b,*]

[a] College of Management, MingDao University, 369 Wen-Hua Road, Peetow, ChangHua 52345, Taiwan
[b] Institute of Traffic and Transportation, National Chiao Tung University, 4F, 118 Sec. 1, Chung Hsiao W. Road, Taipei 10012, Taiwan

Received 3 March 2006; received in revised form 15 June 2007; accepted 18 June 2007

Abstract

The characterization of the dynamics of traffic states remains fundamental to seeking for the solutions of diverse traffic problems. To gain more insights in traffic dynamics in the temporal domain, this paper explored traffic patterns in higher-dimensional state spaces, where we attempted to map the one-dimensional traffic series into appropriate multidimensional spaces by Takens' algorithm. After such a state space reconstruction, we then made use of the largest Lyapunov exponent to depict the rate of expansion or contraction of traffic state trajectories in the reconstructed spaces. The correlation dimension was further estimated to examine if the traffic state trajectories exhibited chaotic-like or stochastic-like motions. An empirical study using flow, speed, and occupancy time-series data as well as the speed-flow, speed-occupancy, and flow-occupancy paired data collected from dual-loop detectors on a freeway of Taiwan was conducted. The numerical results revealed that different nonlinear traffic patterns could emerge depending on the observed time-scale, history data and time-of-day. In addition, with consideration of sequential order and spatiotemporal features, more information about traffic dynamical evolution was extracted.

Keywords: Dynamical behavior; Reconstructed state spaces; Temporal traffic pattern; Traffic state trajectory

1. Introduction

Traffic patterns are those characteristics of vehicle groups passing a point or short segment during a specified span or traveling over longer sections of highway. Various applications of cooperative driving or any kind of driver information and assistance systems are strongly dependent on actual and predicted traffic patterns. In terms of temporal features, traffic time series data measured in different time scales or intervals serve

* Corresponding author. Tel.: +886 2 2349 4958; fax: +886 2 2349 4953.
E-mail addresses: lawrencelan@mail.nctu.edu.tw (L.W. Lan), jbsheu@mail.nctu.edu.tw (J.-B. Sheu), touchme@webmail.tcpd.gov.tw (Y.-S. Huang).
[1] Tel.: +886 4 887 6660; fax: +886 4 887 9014.
[2] Tel.: +886 2 2349 4963; fax: +886 2 2349 4953.

0968-090X/$ - see front matter
doi:10.1016/j.trc.2007.06.006

different purposes. In planning, for instance, one might wish to estimate the annual traffic volume over the planned horizon for proposed infrastructure alternatives. The annual volume is then used for estimating the expected saving in travel time for economic feasibility studies. For design purposes, however, hourly traffic volume is often required to determine the facilities' capacity. Thus, accurately predicting the hourly flow variations would become essential to avoid an over- or under-design of new facilities. For operational purposes, much shorter-term traffic information, such as minute-flow, is essential for real-time traffic management and control. In addition to flow, other traffic data in temporal perspectives such as occupancy and speed are also crucial for various practical purposes.On the other hand, traffic occurs in space and time, i.e., spatiotemporal features. If we explore the spatiotemporal traffic patterns, more insightful information may provide us an understanding of freeway traffic that can be used for effective traffic management, traffic control, organization and other engineering applications, which should increase freeway capacity, improve traffic safety and result in high-quality mobility. In particular, surveying the congested traffic patterns could give us necessary information for efficient collective management strategies, including such well-know methods as ramp metering and traffic assignment. Varaiya (2005) pointed out that effective management on highway congestion through investigation of traffic patterns can significantly reduce congestion. As such, disclosure of the freeway traffic patterns deserves in-depth exploration.

Most of the early paradigms have employed stochastic processes to depict the traffic time series by using some presumed mathematical (probabilistic) distributions. Taking headways as an example, May (1990) categorized their features into random, constant, and intermediate states. Wherein, headways categorized as the intermediate case is the most difficult to model, although it is the most frequently encountered case in a real-world situation. Likewise, traffic flows are often modeled by different stochastic processes. For instance, Poisson distributions are widely acknowledged in low-volume conditions where the mean and the variance of counting traffic are about the same. Such traffic conditions can be associated with random headway states. In contrast, binomial distributions are often utilized for near-capacity conditions where the mean of flow rates is typically larger than its variance. These traffic conditions correspond to nearly constant headway states. The intermediate flow count between these two boundary states can be very complex, and has been modeled by different probabilistic distributions. In the late 1970s, autoregressive integrated moving average (ARIMA) processes had become very popular in the study of linear stochastic time series (Box et al., 1976; Jenkins and Alavi, 1981). Moreover, a large amount of literature has extended analytical tasks from pure time series models to dynamically generalized linear models (Ansley et al., 1977; Clarke, 1983; Maravall, 1983; Liu and Lin, 1991; Chang and Miaou, 1999; Lee and Fambro, 1999; Lingras et al., 2000; Williams, 2001; Williams and Hoel, 2003), and to multivariate time-series state space models (Stathopoulos and Karlaftis, 2003) assuming that the dynamics of traffic flow may follow a linear system or can be modeled with a time invariant linear filter by Wold's decomposition.

A certain number of previous studies also have aimed at the trajectories of traffic patterns varying in the spatial domain for specific purposes such as geometric design of traffic systems and advanced traffic control. Such spatial traffic patterns, which vary transversely across the highway between lanes and direction of travel and longitudinally along the highway or street, may also provide useful information for control and design purposes, such as incident detection, accident investigation, roadway design, etc. For example, Sheu et al. (2004) presented a discrete-time nonlinear stochastic model to characterize the traffic states under the condition of lane-blocking incidents on surface street. In the late 1990s, a "three-phase traffic theory" was developed to depict the spatiotemporal traffic patterns (Kerner, 1998, 1999, 2002a,b). Subsequently, several models, including Kerner–Klenov model, CA model, FOTO and ASDA models, were presented to recognize and track traffic breakdown and spatiotemporal congested patterns (Kerner and Klenov, 2002; Kerner et al., 2002, 2004). In addition, Kerner (2004) and Kerner et al. (2006) further pointed out a few drawbacks of fundamental diagram approaches in describing of spatiotemporal congested freeway patterns. By Kerenr's three-phase traffic theory, the spatiotemporal relationship among traffic variables has been elaborately illustrated.

Other paradigms treat traffic series as a nonlinear system. For instance, Disbro and Frame (1989) utilized chaos theory, a nonlinear system with aperiodic determinism, to describe traffic flow phenomena, and Dendrinos (1994), Zhang and Jarrett (1998), Lan et al. (2003) and Shang et al. (2005) in their analysis of traffic data also found that chaotic characteristics exist in traffic systems. In addition, Smith et al. (2002) stated that the presence of "chaotic like" behavior cannot be completely dismissed, especially during congestion when traffic

flow is unstable and a stronger causative link may be operating in the time dimension. In reality, at times it is very difficult to make such a spatiotemporal analysis of empirical data extracted from "isolated" stationary detectors. Under such restriction – only temporal traffic patterns were investigated, nonlinear phenomena such as equilibrium (stable) fixed points, periodic, quasi-periodic motions or chaotic characteristics, and stochastic or random behaviors could be analyzed in a traffic dynamical system. Therefore, it may not be appropriate to view any traffic series as a pure deterministic or complete random time-series. Instead, traffic flow dynamics may be characterized in a comprehensive spectrum featured in the range between random and deterministic. Only through sufficient evidence from field observations can we be sure of the dynamical behaviors of traffic series, thereby in turn, enabling modeling (elucidating or predicting) the traffic series in a more accurate manner for practical applications.

In view of the scarcity of information provided by one-dimensional traffic time-series, and the lack of considering sequential order in fundamental diagrams proposed by traffic stream models, the main objective of this study was to characterize evolutional state trajectories in appropriately reconstructed state spaces and chronological relationship for paired- and three-traffic variables in multiple dimensions at an isolated station as well as between two nearby stations. From successive days with coarse scales to within a day using subtle observation (20-s, 1-min, etc.), then to several days with different time intervals, we have attempted to gain in-depth insights into the evolution of traffic time-series. By investigating the temporal patterns of traffic dynamics in reconstructed state spaces, we can understand the characteristics of traffic series and further develop effective managements, such as incident detection, extended delay prevention and ramp metering other than those known in one-dimensional space. Furthermore, a close look at traffic time-series not only provides useful information for application in ITS, but improves upon the shortage of linear models for conventional stochastic processes. Aside from the above temporal patterns, we believe that this analysis may have a sense as the first step for understanding of complex behavior of spatiotemporal features of congested traffic patterns. The following content of the paper begins with the description of our rationales for methodology development, followed by a brief of data acquisition and discussion of analytical results. We conclude with an elaboration of the research and suggestions for future research.

2. Reconstruction of state spaces

Reconstruction of state spaces involves two main steps: (1) determination of appropriate time delay and (2) embedding dimension. In the study, the fundamentals of Takens' method were utilized to determine appropriate time delay. Note that Takens' method has been extensively applied to many disciplines of science and engineering (Abarbanel, 1996; Kants and Schreiber, 2004). In Takens (1981), it was proved that, under fairly general conditions, the underlying dynamical system could be faithfully reconstructed from time series, in the sense that a one-to-one correspondence can be established between the reconstructed and the true but unknown dynamical systems. Details about the developmental procedures and rationales for state space reconstruction were depicted in the following, including determination of time delay, embedding dimension and how to measure the motion of trajectories in reconstructed spaces via largest Lyapunov exponent and attractor dimension.

2.1. Determination of time delay

First, let us specify a dynamic system to elaborate traffic dynamics and its properties. In the study, traffic dynamics (including flow, speed and occupancy) is named interchangeably as traffic time series or traffic series referring to the temporal evolution of any traffic variable or its state trajectories measured in a chronological sequence with equal time interval. Now, let $x(t)$ denote the traffic series describing the time evolution in phase space, then it can be expressed by on ordinary differential equation $\dot{x}(t) = F(x(t))$, $t \in R$; or in discrete time $t = n\Delta t$ by maps of the form $x_{n+1} = f(x_n)$, $n \in Z$, where x is a state vector that is finite dimensional $x \in R^n$, and f and F are referred to as vector fields explicitly depending on n and t. The space R^n in which x evolves is called a state space. A traffic time series can also be considered as a sequence of observations $\{S_t = s(x_n)\}$ performed with some measurement function $s(\cdot)$, wherein the one-dimensional traffic time series embedded into multiple dimensions reconstructed spaces is denoted as $S_t = (s_t, s_{t+\tau}, s_{t+2\tau}, \ldots, s_{t+(m-1)\tau})$, $t = 1, 2, \ldots, N$

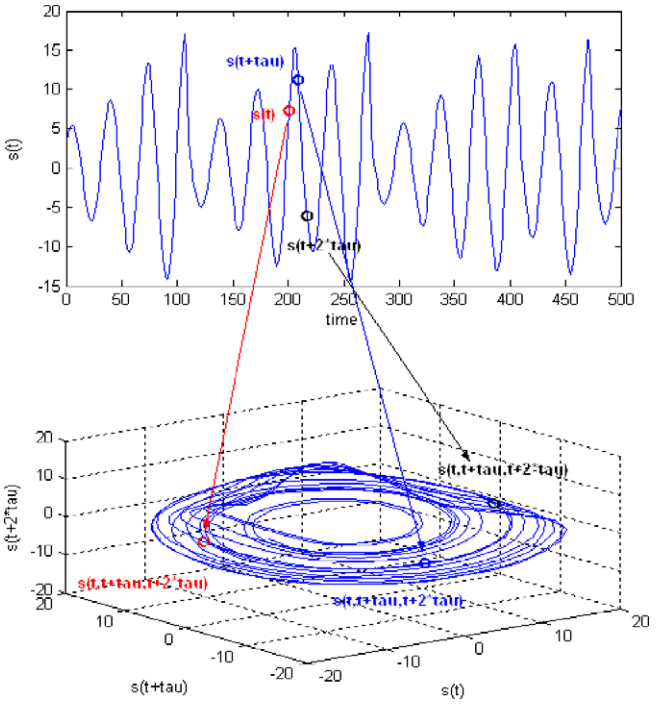

Fig. 1. The concept of traffic series time delay in 1-D and 3-D spaces.

where the parameter τ is called time delay and the integer m is called embedding dimension. In space, geometric objects with non-integer dimensions are called fractals, whereas a geometric object, which characterizes the long-term behavior of a system in the phase space, is called an attractor. Correlation dimension is a measure of the extent to which the presence of a data point affects the position of the other point lying on the attractor.

Accordingly, time delay for any traffic series can be conceptualized with Fig. 1. In the top panel, the red, blue and black circles[3] represent the value of series at time t; $t+\tau$ and $t+2\tau$ respectively; in contrast to the low panel, one can find their corresponding circles in the multidimensional spaces through reconstruction. If the time delay is different, the portrait in multidimensional spaces will change immediately. Thus, it is important to decide a proper time delay when one map a time series into a multidimensional space, that is the quality of reconstructed portraits for a traffic time series depends on the value of τ. For small τ, s_t and $s_{t+\tau}$ are very close to each other, whereas for a large value of τ, s_t and $s_{t+\tau}$ can be completely independent of each other, and any connection between them is random. Consequently, we need a criterion for an intermediate choice that is large enough so that s_t and $s_{t+\tau}$ are independent but not completely independent in a statistical sense.

There are two alternatives to estimate the time delay required by the embedding theorem from an observed traffic time series. The first one is calculating the linear autocorrelation function (ACF) of the data points and selecting τ as the time of its first zero-crossing. The rationale behind this approach is that the time when ACF reaches a zero value marks the point beyond which the $s_{t+\tau}$ sample is completely de-correlated from s_t. However, this approach is suitable only for linear time series. The second one involves the calculation of data from a nonlinear autocorrelation function called average mutual information (AMI), which is proposed by Fraser and Swinney (1986) and can be expressed as θ_{ij} in Eq. (1):

$$\theta_{ij} = -\sum_{i,j} p_{ij}(\tau) \ln \frac{p_{ij}(\tau)}{p_i p_j} \tag{1}$$

where for some partition on the real numbers, p_{ij} is the probability of finding a time series value in the ith interval, and $p_{ij}(\tau)$ is the joint probability that an observation falls into the ith interval and an observation time

[3] For interpretation of the references to color in Fig. 1, the reader is referred to the web version of this article.

τ later falls into the jth interval. In theory, this expression has no systematic dependence on the size of the partition elements and can be quite easily computed. There exist good arguments that if the time delayed mutual information exhibits a marked minimum at a certain value of τ, then this is a good candidate for a reasonable time delay. In practice, one may not be interested in the absolute values of mutual information but rather in its first minimum, and thus the first minimum of AMI usually signal a proper time delay for the time series. Compared with ACF that only measures linear correlations, AMI also takes into account nonlinear correlations, therefore this paper will use the AMI approach by Fraser and Swinney (1986) to determine the proper time delay for traffic time series.

2.2. Determination of embedding dimension

The purpose of the reconstructed state spaces is to find an Euclidean space that is large enough so that the set of points describing the attractor can be unfolded without ambiguity. Kennel et al. (1992) proposed a false nearest neighbor (FNN) algorithm to determine the minimal sufficient embedding dimension m. The FNN algorithm is to search for point s_i in the time series and to look for its nearest neighbor s_j in an m-dimensional space, followed by calculating the distance $\|s_i - s_j\|$ and iterating both the points, and then computing the ratio $\varepsilon_{i,j}$ of Eq. (2) in an m-dimensional space.

$$\varepsilon_{i,j} = \frac{|s_i^{m+1} - s_j^{m+1}|}{\|s_i^m - s_j^m\|}, \ldots i, j = 1, 2, \ldots, N \tag{2}$$

If the ratio $\varepsilon_{i,j}$ exceeds a given heuristic threshold ε_t, this point s_i is marked as having a false nearest neighbor, wherein in general, the value of the threshold ε_t is recommended as lying between 10 and 15 (Nayfeh and Balachandran, 1995; Abarbanel, 1996). The criterion that the embedding dimension is high enough is that the fraction of points for which $\varepsilon_{i,j} > \varepsilon_t$ is zero, or at least sufficiently small.

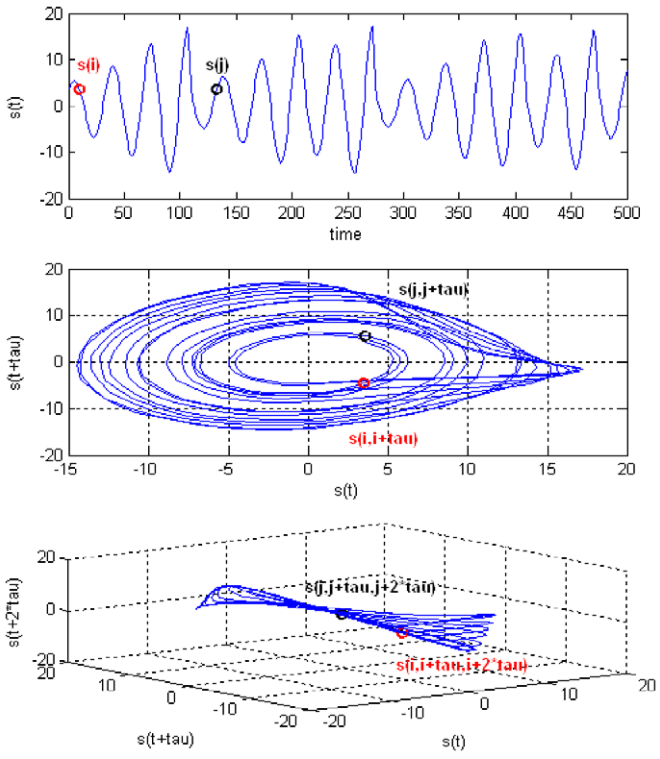

Fig. 2. The concept of measuring the distance of traffic time series by FNN algorithm.

Fig. 2 illustrates an example depicting the FNN algorithm. In the top panel, the black circle is the nearest point to the red circle[4] within 500 points in one-dimension, wherein their Euclidean's distance is 0.02. A simple method is used to project the red circle and the black circle to the y-axis, whereafter it is apparent that the distance between the two circles is very close. However, the value becomes 10.01 if one calculates the Euclidean distance in a two-dimensional plane (middle panel) according to proper time delay. Because the ratio of 10.01 divided by 0.02 is greater than the threshold, ε_t, thus, the black circle is a false neighbor of the red circle. If one further calculates the ratio of distances between a two-dimensional plane and a three-dimensional space (low panel), then it demonstrates that the ratio dropped drastically because the Euclidean distance is 10.4 in the three-dimensional space. Since the ratio is no longer greater than the threshold, ε_t, it suggests that an embedding dimension of $m = 2$ is sufficient. After we examine every point in this time series according to the above algorithm, the proper embedding dimension can be decided. However, if there are a multitude of identical values in a realistic time series, then FNN algorithm probably cannot work precisely. In that case, the embedding dimension would be determined approximately by correlation dimension instead.

3. Motions of traffic state trajectories

Once the appropriate time delay and embedding dimension for a traffic series are determined, one can map the one-dimensional traffic series into m-dimensional reconstructed spaces. After that, one is interested in knowing how traffic state trajectories moved in this space over time. Note that traffic state trajectories in this paper refer to traffic variables (flow, time-mean-speed, percent occupancy), which were tracked and recorded in reconstructed state spaces over time rather than vehicles changing their position with time evolution. This paper makes use of the Lyapunov exponent to measure the rate of expansion or contraction of traffic state trajectories and is described hereinafter.

3.1. Estimation of the largest Lyapunov exponent

If we take two points s_i and s_j in the reconstructed spaces, and indicate the distance between them as $|s_i - s_j| = \delta_0$, then, after a time span Δt, it is expected that the new distance δ will be equal to $\delta = \delta_0 e^{\lambda \Delta t}$, where λ is called the Lyapunov exponent. For an m-dimensional space, the rate of expansion or contraction of trajectories is described for each direction by one Lyapunov exponent, resulting in m different λs. Of the m different λs, the largest value λ_0 (largest Lyapunov exponent) is of main interest since it can be easily calculated even without the explicit construction of a model for the traffic time series. If λ_0 is negative, the traffic state trajectories will converge to a fixed point. If λ_0 is zero, the traffic state trajectories are periodic motions. If λ_0 is positive, the traffic state trajectories may exhibit other motions such as an aperiodically deterministic chaos or stochastic randomness (Hilborn, 2000; Kants and Schreiber, 2004).

In theory, the largest Lyapunov exponent can be used to identify the traffic state trajectories moving in the reconstructed state spaces. However, in practice, there will be fluctuations in the calculation of the largest Lyapunov exponent due to noisy traffic data. For instance, in a true state space, distances do not always grow everywhere on the attractor at the same rate, and in fact they may even shrink locally. To minimize the influence of noisy field traffic data on calculating the largest Lyapunov exponent, one can employ an appropriate averaging statistic when computing the average exponential growth of distance. To realize this, the following procedures are proposed: (1) choosing a point s_i of the traffic time series in the reconstructed spaces and select all neighbors with a distance smaller than r. (2) Computing the average over the distance of all neighbors to the reference part of the trajectories as a function of the relative time. The logarithm of the average distance at time t is some effective expansion rate over the time span Δt (plus the logarithm of the initial distance) containing all the deterministic fluctuations due to projection and dynamics. (3) Repeating this for many values of i, thereby averaging out the fluctuations of the effective expansion rates (Kants and Schreiber, 2004).

The above procedures can be represented as Eq. (3), wherein the curves of stretching factor $\zeta(\Delta t)$ exhibit a robust linear increase, slope of which is an estimate of the largest Lyapunov exponent λ_0 per time step.

[4] For interpretation of the references to color in Fig. 2, the reader is referred to the web version of this article.

$$\zeta(\Delta t) = \frac{1}{N}\sum_{i=1}^{N} \ln\left(\frac{1}{|\Psi(s_i)|}\sum_{s_j\in\Psi(s_i)} |s_{i+\Delta t} - s_{j+\Delta t}|\right), \quad i,j = 1,2,\ldots,N \tag{3}$$

where $\Psi(s_i)$ is the neighborhood of s_i with diameter r.

3.2. Estimation of the correlation dimension

Correlation dimension is a measure of the extent to which the presence of a data point affects the position of other points lying on the attractor. Among the number of methods available for distinguishing between chaotic motions and stochastic motions of a time series trajectories, the correlation dimension is perhaps the most fundamental one (Shang et al., 2005). A seemingly irregular phenomenon arising from any deterministic time series dynamics will have a limited number of degrees of freedom equal to the smallest number of first-order differential equations that capture the most important features of the time series. Thus, when one reconstructs spaces with increasing dimensions for an infinite data set, a point will be reached where the dimensions are equal to the number of degrees of freedom, and beyond which increasing the dimension of the representation will not have any significant effect on the correlation dimension. Under this circumstance, we view the correlation dimension of the attractor as saturated. If the attractor dimension is saturated in low-dimensions (normally, five-dimensions), then it signalizes that the time series trajectories exhibit aperiodic motions, which is essentially deterministic chaos. In contrast, if an attractor dimension cannot reach saturation or is saturated in very high-dimensions, then the trajectories of that time series could be stochastic.

Grassberger and Procaccia (1983) showed that correlation dimension d can be evaluated by using the correlation integral $\mu(r)$, which is the probability that a pair of points (s_i, s_j) chosen randomly in the reconstructed spaces are separated by a distance less than r. If N is the number of points in the reconstructed vector time series S_t, the correlation integral can be approximated by the following sum in Eq. (4) (Grassberger and Procaccia, 1983):

$$\mu_N(m,r) = \frac{2}{N(N-1)}\sum_{j=1}^{N}\sum_{i=j+1}^{N} \Theta(r - |s_i - s_j|) \tag{4}$$

where Θ denotes the Heaviside step function and $|s_i - s_j|$ stands for the distance between points s_i and s_j; $\Theta(r - |s_i - s_j|) = 0$, if $r - |s_i - s_j| \leqslant 0$ and $\Theta(r - |s_i - s_j|) = 1$, for $r - |s_i - s_j| > 0$. In the limit of an infinite amount of data ($N \to \infty$) and for small r, we expect μ_N to scale like a power law:

$$\mu(m,r) \propto \alpha r^d \tag{5}$$

where α is a constant and d is the correlation dimension or the slope of the $\ln\mu(r)$ vs. $\ln r$ plot given by

$$d = \lim_{r\to 0}\lim_{N\to\infty} \frac{\partial \ln \mu_N(m,r)}{\partial \ln r} \tag{6}$$

To observe whether a time series exhibits deterministic features, the correlation dimension (or local slope) values are plotted against the corresponding embedding dimension values. If the value of the correlation dimension is finite, low and non-integer, then the system is possibly exhibiting as low-dimensional chaos. The saturation value of the correlation dimension is defined as the correlation dimension of the attractor, or so-called attractor dimension. In general, an embedding dimension (m) is no less than double the attractor dimension ($2d$) plus one. In contrast, if the correlation dimension increases without bound with increase in the embedding dimension, then the system is considered as stochastic.

4. Empirical study

To illustrate the proposed model's potential advantages in analyzing traffic dynamics, an empirical study was conducted, where the main procedures of data acquisition and analytical results were provided in the following.

4.1. Data

In this study, traffic time-series were directly extracted from dual-loop detectors installed at a given 3–4-lane mainline segment of the northbound Sun Yat-Sen Freeway of Taiwan, located in the northern area of Taipei County. In order to discover the features of traffic time-series in different situations, we divided the collected raw data into three groups. Data in the first group was counted aggregately by average flow, time-mean-speed and percent occupancy per 5-min per approach. The data was extracted from station N27.9 near station 433, collected from traffic inbounds to Taipei City. Data in the second group contained flow, time-mean-speed and percent occupancy per 20-s per lane recorded in median lane. The data was collected from stations 402, 404, 421 and 433. Stations 402 and 404 are outbound from Taipei City, whereas stations 421 and 433 are inbound to the City. Data in the third group was a processed data set, i.e., we combined 10-workday time-series, which every workday time-series was come from the second group data. Then, we divided the combined time-series into four subgroups according to four time-of-day intervals, i.e., 00:00–03:00, 06:00–09:00, 12:00–15:00 and 18:00–21:00. The purpose of processing the traffic time-series was to compare different features of traffic series between four time-of-day intervals. Similarly, in order to examine the features between traffic time-series with various time scales, in the second group, we further accumulated the 20-s traffic series into longer-term data, including 1-min, 3-min and 9-min series, of which, flows were directly summed from each 20-s flow, speeds were the weighted average of each 20-s time-mean-speed multiplied by its corresponding flow and occupancies were the arithmetic mean of each 20-s occupancy. Likewise, in the first group, the 5-min approach data sets were accumulated into 15-min, 30-min and one hour time-series via the above method. In addition, variation in the traffic time-series is similar for the three groups and the traffic patterns change on different days, but never exactly repeat. Fluctuations in the 20-s time series is the most severe, as the measured time interval gets larger, the degrees of variation decline. It is noted that the traffic series extracted from "isolated" stations can only provide us to explore the temporal patterns of traffic dynamics, not spatiotemporal features over several adjacent segments. This is the restriction of our empirical investigation.

4.2. Higher-dimensional traffic patterns

The following demonstrates more interesting features of our empirical traffic series mapped in a reconstructed state space. First, the 20-s traffic series for a typical workday at station 433 is reconstructed into

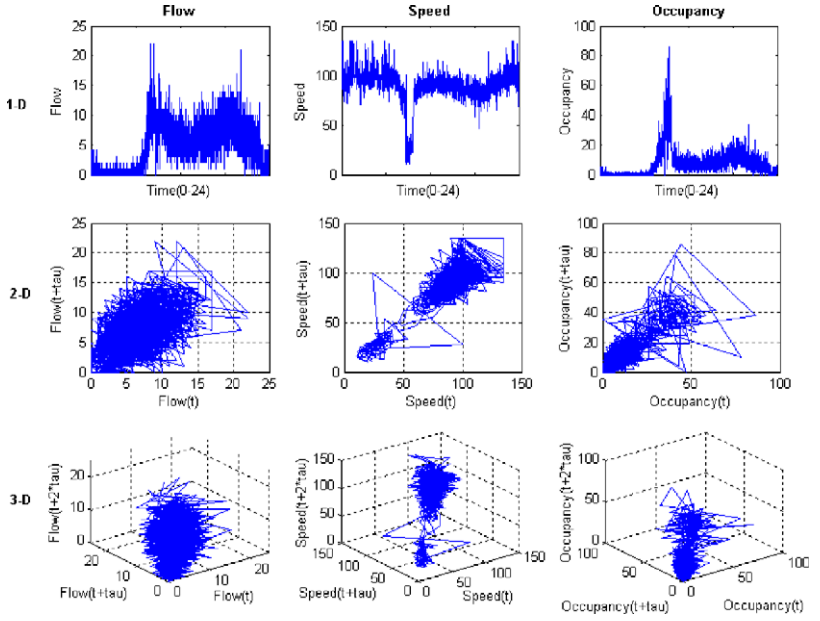

Fig. 3. Comparison of 1-D, 2-D and 3-D 20-s traffic series on a typical workday (station 433).

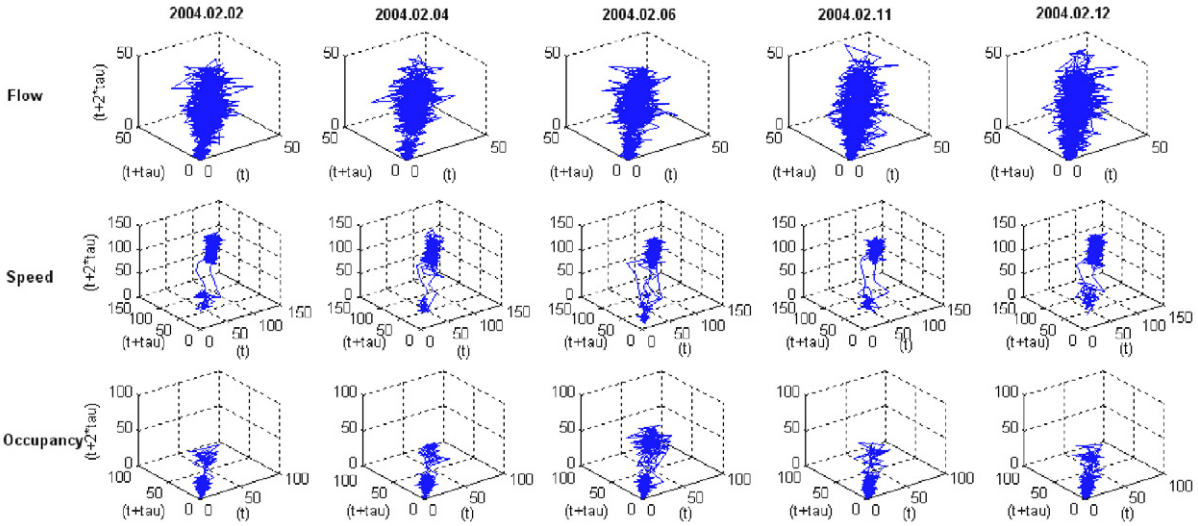

Fig. 4. Three-dimensional 1-min traffic series for five workdays (station 433).

two- and three-dimensional state spaces with appropriate time delays. Fig. 3 compares the same traffic series plotted in 1-D, 2-D and in 3-D spaces. With reference to time delay, it can be seen that points in 1-D numerically change with time evolution, while in the 2-D diagram points not only change with time evolution but also composed of s_t and $s_{t+\tau}$. Similarly, in the 3-D diagram every point is composed of s_t, $s_{t+\tau}$ and $s_{t+2\tau}$. Consequently, variation in 1-D correspond to the degree of spread in 2-D and 3-D spaces, in addition, the steep fluctuations in 1-D correspond to different areas in 2-D or in 3-D spaces. On the other hand, the state trajectories in the 2-D and 3-D diagrams change with time enabling the state trajectories to move back and forth. However, the curves always move forward with time.

Fig. 4 presents the three-dimensional 1-min traffic series for five workdays at station 433. The different features of traffic series in three-dimensional spaces from day to day are similar but not exactly the same. To see the effect of time scale, Fig. 5 demonstrates the traffic patterns in three-dimensional reconstructed state spaces measured in 20-s, 1-min, 3-min and 9-min intervals respectively for one workday at station 433. It is noticed

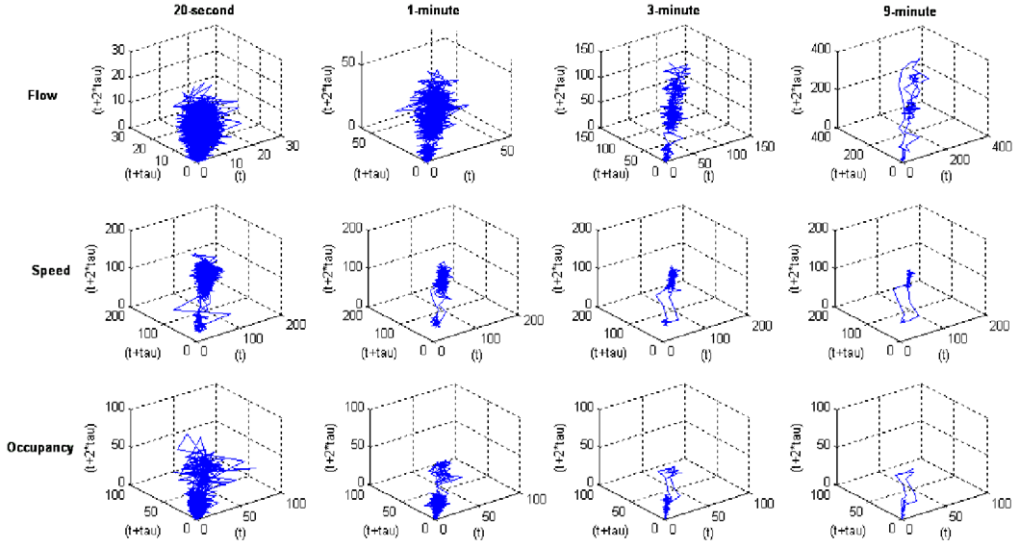

Fig. 5. Three-dimensional traffic series measured in various time scales (station 433).

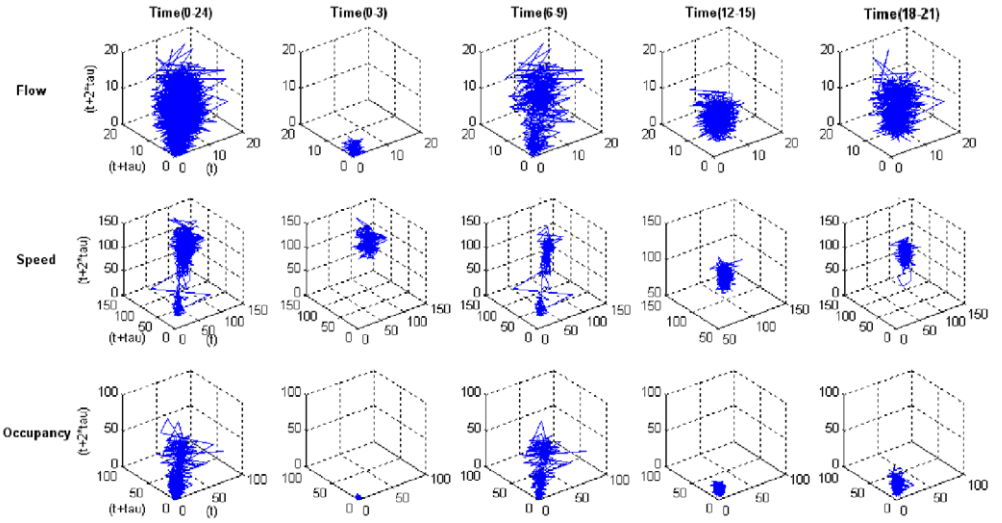

Fig. 6. Three-dimensional 20-s traffic series in different times of day (station 433).

that the traffic features become more explicit as the time scale gets coarser. Fig. 6 further compares the features of 20-s traffic series over 24 h and within various times of day arranged from midnight to evening peak-hour period, i.e., 00:00–03:00, 06:00–09:00, 12:00–15:00 and 18:00–21:00. Investigating the dynamical behaviors at different times of day, one can find that the conspicuous dynamics of traffic state trajectories come mainly from periods 06:00–09:00 and 18:00–21:00. In the early hours, when traffic is very calm, the occupancy trajectories shrink to very low values, but the speed trajectories can vary rather significantly, which fully explains heterogeneous driver characteristics. Under free flow conditions, some aggressive drivers may move very fast while some conservative drivers may not, causing the wide diversity of speed dynamics. In contrast, during the morning peak-hour period, speed trajectories tend to shrink to some low values while flow trajectories can vary largely in a wide-range domain.

4.3. Illustrations of traffic state trajectory evolution

Let us take the 9-min traffic series as an example to further explore the dynamical behaviors of trajectories in more detail. In order to trace the sequential order, we only illustrate a limited number of points of the dynamics, as shown in Fig. 7, which clearly indicates the dynamical behaviors of state trajectories in the reconstructed spaces. For a typical workday, the flow state trajectories move around the lowest corner, i.e., at the coordinate (0, 0, 0) with less fluctuation at midnight (00:00–03:00). In the morning peak-hours (06:00–09:00), however, the state trajectories advance along the diagonal direction and sometimes move back and forth as time evolves, which continue to advance until the later morning peak-hours. During off-peak-hours (12:00–15:00), the state trajectories fluctuate in the middle of the 3-D spaces. After evening peak-hours (18:00–21:00), the state trajectories move back to the original place. The whole sequence of features of the traffic flow series within a day are demonstrated in Fig. 8, which similarly shows that the motion of occupancy trajectories advances along the diagonal direction from bottom to top in the reconstructed space. The difference between the occupancy and flow state trajectories is that the range of motion for occupancy is smaller than that for flow. Compared with flow and occupancy, the direction of motion for speed state trajectories is just the opposite, i.e., from top to bottom. It can be concluded that the direction of traffic state trajectories in multidimensional spaces corresponds to the trend of the traffic series in 1-D space, especially when the data is measured on a coarse scale.

Fig. 9 shows a comparison between 1-D and 3-D spaces for successive traffic flow series. In the top panel, the flow series goes from left to right with time evolution while the direction of traffic state trajectories goes anti-clockwise with time evolution in reconstructed spaces. Four data points have been selected and marked

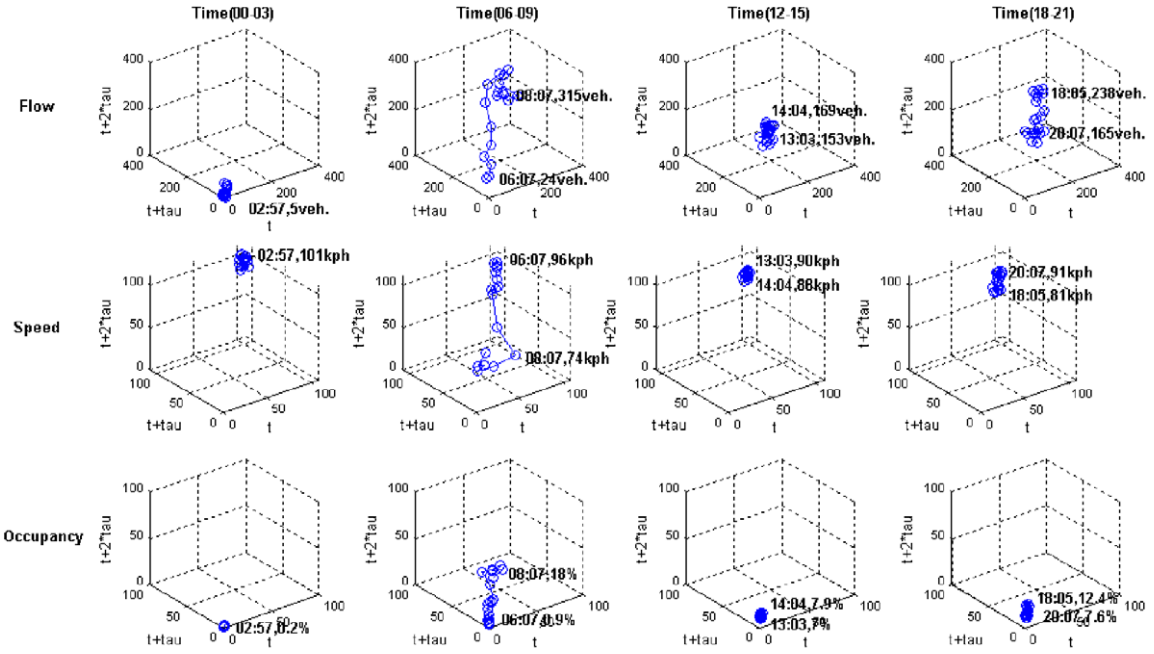

Fig. 7. The dynamics of 9-min traffic trajectories in various time-of-day in 3-D spaces (station 433).

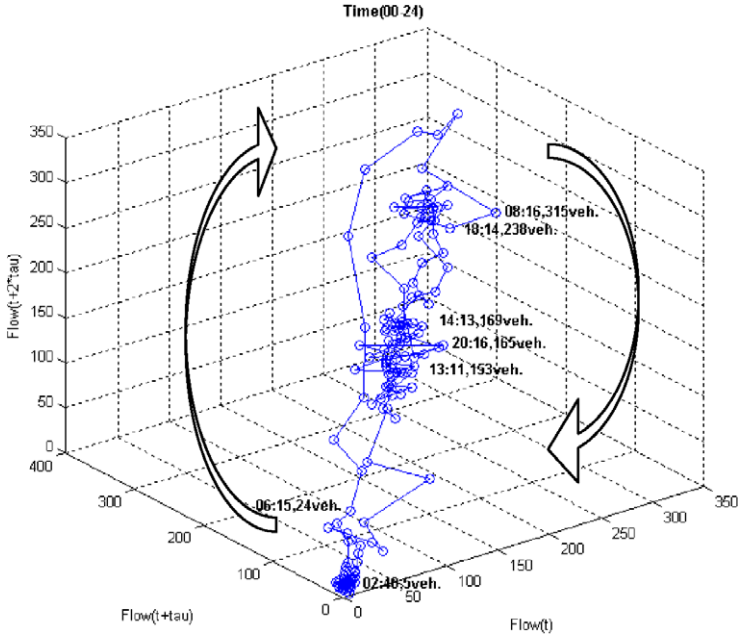

Fig. 8. The whole-day dynamics of 9-min flow trajectories in 3-D spaces (station 433).

with Arabic numerals 1, 2, 3, and 4 in the top panel, wherein time delays between paired points i.e., point 1 vs. point 2; point 3 vs. point 4, are equal. After reconstruction, the four points were projected into the bottom panel and correspondingly marked with the same Arabic numerals 1, 2, 3, and 4. From Fig. 9, it is found that, in the top panel, the difference in flow between points 1 and 2 is lower than between points 3 and 4, therefore, in the bottom panel the distance between points 3 and 4 is larger than between points 1 and 2. In addition, in

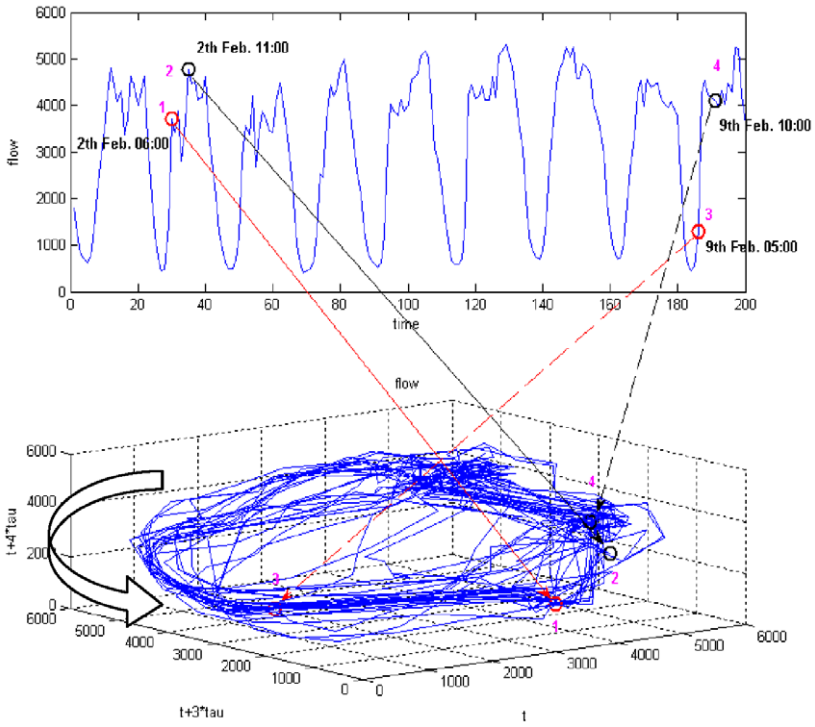

Fig. 9. Successive flow time-series in 1-D and its trajectories in 3-D reconstructed spaces (flow: vehicles per hour per approach).

the bottom panel, one circle distance of trajectories going around the space approximately equals the variety of flow from 00:00 to 24:00 in the top panel. However, it is noticed that not every circle moves smoothly, but heads for one direction with variation and the degrees of variation increase by the time scale shortening.

4.4. Diverse patterns for traffic state trajectories

In this section, we employ the methodologies introduced in Sections 2 and 3 to further compute the related parameters that can disclose the features of traffic series. The results are summarized in Tables 1–5. From Table 1, it is found that the relationship between time delay and time interval is an inverse proportion. The values of embedding dimension are five or six, which illustrate that the successive traffic series are not composed of a disorder data set, but rather, some state trajectories are dominated by an intrinsic attractor, which may be called as a "deterministic-like" feature. Furthermore, the numerals in the last column (correlation dimension) represent attractor dimension changing with embedding dimension increasing. Further observing the tendency for correlation dimension, it is easily noticed that the slope of curve is much smoother with increasing embedding dimension, and as the time scale gets larger, the degree of smoothness becomes more obvious. In addition, although the largest Lyapunov exponents are positive; however, they are almost nearly equal to zero, which means that the successive traffic series in reconstructed spaces should be periodic trajectories or they recur regularly day after day.

From Tables 2 to 4, it is found that the proper embedding dimensions for 20-s flow, speed and occupancy state trajectories are around 9 and 10, which are rather high. It suggests that these 20-s traffic state trajectories exhibit much more stochastic motions than deterministic-like motions, if observed within a typical workday. Furthermore, the reason that the time delays of traffic series on different workdays, stations and time scales are always equal to one is that the AMI exhibits a fairly low value at $(t+1)$ step, then the value does not drop down to zero abruptly at following steps but gradually decrease. In other words, the time delays at $(t+1)$, $(t+2)$, …, $(t+m-1)$ steps are relatively small corresponding to the time delay at $t=0$, thus the time delays (Table 1) can be considered as "one". From Table 3, however, it is found that the proper embedding dimen-

Table 1
Four parameters of successive one-month traffic series

Traffic variable	Time scales	Time delay (τ)	Embedding dimension (m)	The largest Lyapunov exponent	Correlation dimension (d)
Flow	5-min	61	6	0.002	(0.87, 1.64, 2.12, 2.56, 2.85, 3.01, 3.28, 3.36, 3.64, 3.89)
	15-min	20	6	0.002	(0.87, 1.62, 2.06, 2.46, 2.80, 3.17, 3.60, 3.59, 3.87, 3.72)
	30-min	10	5	0.005	(0.88, 1.66, 2.22, 2.72, 2.83, 3.16, 3.44, 3.46, 3.59, 3.72)
	60-min	5	5	0.005	(0.88, 1.65, 2.10, 2.40, 2.46, 2.74, 2.71, 2.86, 2.74, 2.78)
Speed	5-min	84	6	0.001	(0.76, 1.49, 2.17, 2.74, 3.11, 3.33, 3.53, 3.76, 3.96, 4.13)
	15-min	27	6	0.001	(0.79, 1.53, 2.15, 2.58, 3.14, 3.14, 3.18, 3.42, 3.65, 3.89)
	30-min	13	5	0.005	(0.85, 1.64, 2.30, 2.65, 3.02, 3.13, 3.45, 3.72, 3.52, 3.70)
	60-min	6	5	0.005	(0.86, 1.65, 2.17, 2.59, 2.62, 2.75, 2.87, 3.01, 3.16, 3.17)
Occupancy	5-min	61	6	0.002	(0.52, 0.99, 1.38, 1.73, 2.03, 2.25, 2.37, 2.42, 2.45, 2.48)
	15-min	20	6	0.002	(0.70, 1.32, 1.84, 2.23, 2.48, 2.74, 3.14, 3.01, 3.01, 3.11)
	30-min	10	6	0.003	(0.81, 1.51, 2.12, 2.69, 2.55, 2.91, 3.19, 3.05, 3.25, 3.41)
	60-min	5	5	0.005	(0.79, 1.50, 2.07, 2.21, 2.45, 2.43, 2.67, 2.61, 2.76, 2.67)

Table 2
Parameters of 20-s traffic trajectories at different stations on a typical workday

Station	Variable	Time delay (τ)	Embedding dimension (m)	The largest Lyapunov exponent	Correlation dimension (d)
402	Flow	1	10	0.104	Not saturated
	Time-mean-speed	1	9	0.044	Not saturated
	Percent occupancy	1	9	0.101	Not saturated
404	Flow	1	9	0.085	Not saturated
	Time-mean-speed	1	9	0.097	Not saturated
	Percent occupancy	1	9	0.085	Not saturated
421	Flow	1	10	0.112	Not saturated
	Time-mean-speed	1	9	0.066	Not saturated
	Percent occupancy	1	9	0.036	Not saturated
433	Flow	1	10	0.081	Not saturated
	Time-mean-speed	1	9	0.039	Not saturated
	Percent occupancy	1	9	0.021	Not saturated

sions for 1-min flow, speed and occupancy state trajectories are reduced to 6 and 7, lower than those of 20-s measurements, in addition, in Table 4 the proper embedding dimensions have further reduced to 3 or 4 for the 9-min traffic state trajectories, which indicates that an initial deterministic-like pattern would have been observed if the measured time interval gets longer.

From Table 5, the time delays of flow and occupancy, in contrast to those of a typical workday, are no longer equal to one. Instead, like successive time-series, they show different values with various time scales. In addition, the time delay declines with increasing time scale. Such change in time delays from one to specific values indicates that the pattern of traffic series has probably changed. For instance, road users can drive

Table 3
Parameters of 1-min traffic trajectories for five workdays (station 433)

Date	Variable	Time delay (τ)	Embedding dimension (m)	The largest Lyapunov exponent	Correlation dimension (d)
2004. 02.02	Flow	1	7	0.108	Not saturated
	Time-mean-speed	1	6	0.076	Not saturated
	Percent occupancy	1	6	0.067	Not saturated
2004. 02.04	Flow	1	7	0.121	Not saturated
	Time-mean-speed	1	6	0.085	Not saturated
	Percent occupancy	1	6	0.057	Not saturated
2004. 02.06	Flow	1	7	0.134	Not saturated
	Time-mean-speed	1	6	0.085	Not saturated
	Percent occupancy	1	6	0.073	Not saturated
2004. 02.11	Flow	1	7	0.127	Not saturated
	Time-mean-speed	1	6	0.077	Not saturated
	Percent occupancy	1	6	0.075	Not saturated
2004. 02.12	Flow	1	6	0.164	Not saturated
	Time-mean-speed	1	6	0.078	Not saturated
	Percent occupancy	1	6	0.062	Not saturated

Table 4
Parameters of traffic trajectories measured with various time scales on a typical workday (station 433)

Time scale	Variable	Time delay (τ)	Embedding dimension (m)	The largest Lyapunov exponent	Correlation dimension (d)
20-s	Flow	1	10	0.081	Not saturated
	Time-mean-speed	1	9	0.039	Not saturated
	Percent occupancy	1	9	0.021	Not saturated
1-min	Flow	1	7	0.121	Not saturated
	Time-mean-speed	1	6	0.085	Not saturated
	Percent occupancy	1	6	0.057	Not saturated
3-min	Flow	1	4	0.198	Not saturated
	Time-mean-speed	1	4	0.201	Not saturated
	Percent occupancy	1	4	0.120	Not saturated
9-min	Flow	1	4	0.216	Not saturated
	Time-mean-speed	1	3	0.320	Not saturated
	Percent occupancy	1	3	0.273	Not saturated

freely in the early hours as long as they do not speed, i.e., the speed state trajectory is random so that the time delay of speed-series is equal to one; embedding dimension is larger than five; the largest Lyapunov exponent is positive and correlation dimension is not saturated. However, aside from midnight (00:00–03:00), in the morning peak-hours 06:00–09:00, for example, commuters' speeds are mainly confined by heavy traffic volumes, thereby the time delay is no longer equal to one, instead diverse time delays together with evidence of other parameters are exhibited. Hence, we are convinced that the random features must have disappeared.

Apart from time delay, Table 5 also provides additional details regarding embedding dimension. According to the various embedding dimension in Table 5, the characteristics of very short-term traffic time-series (e.g., 20-s and 1-min) seemingly should be stochastic because of relatively high dimensions. In addition, like the successive traffic time-series, parts of the curve for correlation dimension in Table 5 gradually become smooth

Table 5
Parameters of 10-workday traffic trajectories measured in various time scales and intervals (station 433)

	Time interval	Time scale	Time delay	Embedding dimension (m)	λ_0	Correlation dimension
Flow	00:00–03:00	20-s	234	(6–7)	−0.002	(0.4,0.9,1.3,1.7,2.1,2.6,3.0,3.3,3.3,3.3)
		1-min	77	(6–7)	0.003	(0.4,0.8,1.2,1.6,2.0,2.4,2.5,2.8,3.1,3.5)
		3-min	26	(5–6)	0.005	(0.5,0.9,1.3,1.7,2.1,2.6,2.7,2.9,3.0,3.1)
		9-min	9	4	0.009	(0.5,0.9,1.2,1.5,1.6,1.8,1.9,2.1,2.4,2.5)
	06:00–09:00	20-s	129	(10–11)	0.004	(0.8,1.5,2.1,2.7,3.3,3.8,4.3,4.5,4.9,5.5)
		1-min	42	(8–9)	0.006	(0.8,1.6,2.2,2.8,3.4,3.8,4.0,4.5,4.7,4.8)
		3-min	14	5	0.009	(0.8,1.5,2.1,2.4,2.6,2.8,2.8,3.0,3.2,3.4)
		9-min	4	4	0.010	(0.8,1.4,1.9,2.0,2.4,2.6,2.7,2.8,3.1,3.3)
	12:00–15:00	20-s	246	(12–13)	0.002	(0.7,1.4,2.0,2.6,3.3,3.9,4.6,5.1,5.4,6.0)
		1-min	82	(10–11)	0.005	(0.8,1.6,2.3,2.8,3.3,3.6,4.4,4.7,4.8,5.3)
		3-min	28	(8–9)	0.011	(0.8,1.6,2.4,3.1,3.9,4.0,4.4,4.6,4.7,4.9)
		9-min	10	(8–9)	0.014	(0.9,1.8,2.6,3.2,3.6,3.9,4.1,4.1,4.2,4.4)
	18:00–21:00	20-s	182	(10–11)	0.005	(0.7,1.5,2.2,2.9,3.3,4.0,4.3,4.5,5.1,5.6)
		1-min	62	(10–11)	0.007	(0.8,1.6,2.4,3.1,3.6,4.3,4.6,4.8,5.2,5.3)
		3-min	21	7	0.009	(0.9,1.7,2.2,2.5,2.8,2.9,3.2,3.3,3.6,3.7)
		9-min	7	6	0.012	(0.8,1.5,2.0,2.2,2.5,2.7,2.8,3.1,3.3,3.5)
Speed	00:00–03:00	20-s	1	12	0.02	Not saturated
		1-min	1	8	0.08	Not saturated
		3-min	1	6	0.04	Not saturated
		9-min	1	5	0.05	Not saturated
	06:00–09:00	20-s	115	8	0.006	(0.6,1.2,1.7,2.3,2.8,3.3,3.8,4.1,4.4,4.5)
		1-min	38	6	0.007	(0.6,1.1,1.6,2.1,2.6,3.1,3.4,3.5,3.6,3.9)
		3-min	13	5	0.008	(0.6,1.1,1.5,2.0,2.4,2.7,2.8,2.9,3.0,3.0)
		9-min	5	5	0.009	(0.6,1.0,1.3,1.6,1.9,2.1,2.2,2.2,2.2,2.2)
	12:00–15:00	20-s	92	10	0.001	(0.5,0.9,1.4,1.8,2.3,2.8,3.2,3.6,4.0,4.6)
		1-min	32	7	0.003	(0.5,0.9,1.3,1.7,2.2,2.6,3.0,3.3,3.7,4.0)
		3-min	10	6	0.005	(0.4,0.7,1.0,1.4,1.7,2.0,2.3,2.6,2.7,2.8)
		9-min	5	5	0.006	(0.3,0.6,0.8,1.1,1.3,1.5,1.6,1.9,2.1,2.2)
	18:00–21:00	20-s	149	10	0.009	(0.7,1.4,2.1,2.8,3.5,4.1,4.8,5.0,5.6,5.8)
		1-min	60	8	0.013	(1.0,1.4,2.1,2.8,3.6,4.2,4.7,5.0,5.2,5.6)
		3-min	20	4	0.028	(0.8,1.6,2.4,3.2,3.8,4.1,4.6,4.9,5.2,5.5)
		9-min	8	4	0.029	(0.8,1.8,2.7,3.5,3.7,4.1,4.,0,4.1,4.2,4.2)
Occupancy	00:00–03:00	20-s	231	(7–8)	−0.001	(0.6,0.9,1.5,1.9,2.2,2.7,3.2,3.2,3.2,3.2)
		1-min	77	(7–8)	0.003	(0.5,0.8,1.4,1.7,2.1,2.5,3.0,3.2,3.5,3.7)
		3-min	26	(6–7)	0.004	(0.5,0.8,1.4,1.7,2.3,2.6,3.1,3.2,3.5,3.9)
		9-min	9	5	0.010	(0.5,0.8,1.4,1.6,2.2,2.8,2.9,3.1,3.4,3.8)
	06:00–09:00	20-s	115	(8–9)	0.004	(0.8,1.6,2.2,2.6,3.3,3.7,4.1,4.3,4.6,4.9)
		1-min	39	(7–8)	0.006	(0.8,1.6,2.2,2.8,3.4,3.8,3.9,4.3,4.7,4.8)
		3-min	13	6	0.011	(0.8,1.5,2.4,2.7,3.2,3.3,3.3,3.4,3.5,3.6)
		9-min	5	5	0.013	(0.7,1.4,1.8,2.2,2.5,2.8,3.0,3.0,3.1,3.3)
	12:00–15:00	20-s	89	(8–9)	0.002	(0.7,1.4,1.7,2.2,2.3,2.8,3.4,3.7,3.9,4.0)
		1-min	30	(6–8)	0.004	(0.8,1.5,1.8,2.2,2.4,2.6,3.2,3.4,3.4,3.5)
		3-min	10	5	0.009	(0.8,1.4,1.7,2.1,2.3,2.5,2.6,2.8,3.1,3.4)
		9-min	5	4	0.010	(0.6,0.8,1.6,1.8,2.3,2.4,2.6,2.6,2.6,2.7)
	18:00–21:00	20-s	182	(9–10)	0.009	(0.7,1.5,2.2,2.5,3.2,3.4,3.6,3.8,3.9,4.2)
		1-min	60	6	0.011	(0.8,1.5,1.8,2.4,2.6,2.8,3.4,3.6,3.8,3.9)
		3-min	20	5	0.02	(0.8,1.6,1.9,2.3,2.5,2.7,3.2,3.3,3.6,3.7)
		9-min	7	5	0.02	(0.6,1.3,1.6,1.8,2.2,2.5,2.6,2.8,2.8,2.9)

with increasing embedding dimension, which indicates that an initial attractor has been developing to make correlation dimension be saturated. Finally, the negative values of λ_0 for flow and occupancy in the early

hours suggest that flows and occupancy at such times measured in 20-s intervals should be equivalent to fixed point under steady state. Such pattern could result from the fact that traffic flow and occupancy are so lulled (very few travelers going into City) that the state trajectories eventually converge to fixed points in reconstructed state spaces.

5. Some observed details for paired- and three-variable traffic evolutions

The above empirical study has not only demonstrated the traffic patterns by mapping the 1-D traffic series into 3-D state spaces, but has also estimated the most appropriate time delay and embedding dimensions for real-world traffic series. Apart from these, the present paper further compares the paired (speed-flow, speed-occupancy, and flow-occupancy) traffic features with and without relation to the sequential order. Fig. 10 illustrates the 9-min paired-traffic features on a typical workday (station 421). From the upper panel (without sequential order), one can at most figure out the relationships between speed-flow, speed-occupancy and flow-occupancy. However, these relationships do not explain the detailed evolution of traffic behaviors. From the lower panel (with sequential order), in contrast, we can trace the detailed evolution of traffic behaviors. Obviously, sequential order is taken into consideration and more detailed information on traffic evolution dynamics can be found, which could help understand the possible causes of formation of congested traffic phase in such a way that one could propose more effective traffic managements, e.g., regulation of low-speed vehicles in free-flow phase, determination of start-up for ramp metering, and so on.

To illustrate the more detailed information, we trace some selected points to elucidate the daily evolution of the 9-min paired-traffic by observing the chronological order of speed-flow diagram. We start with the first point in the early hours at time 01:12 (flow: 7 vehicles/9-min, speed: 101 kph) at the upper left corner indicating a free traffic phase. As time evolves, the dynamics of speed-flow advances along a southeast direction to the second point in the morning peak hours at time 08:25 (289 vehicles/9-min, 80 kph), which moves southbound to the third point near noon at time 11:58 (313 vehicles/9-min, 60 kph) indicating a congested traffic phase. After that, the dynamics moves back and forth in the middle of diagram, representing phase transitions, during the day-time off-peak-hours, e.g., the fourth point at time 15:12 (129 vehicles/9-min, 87 kph). After the

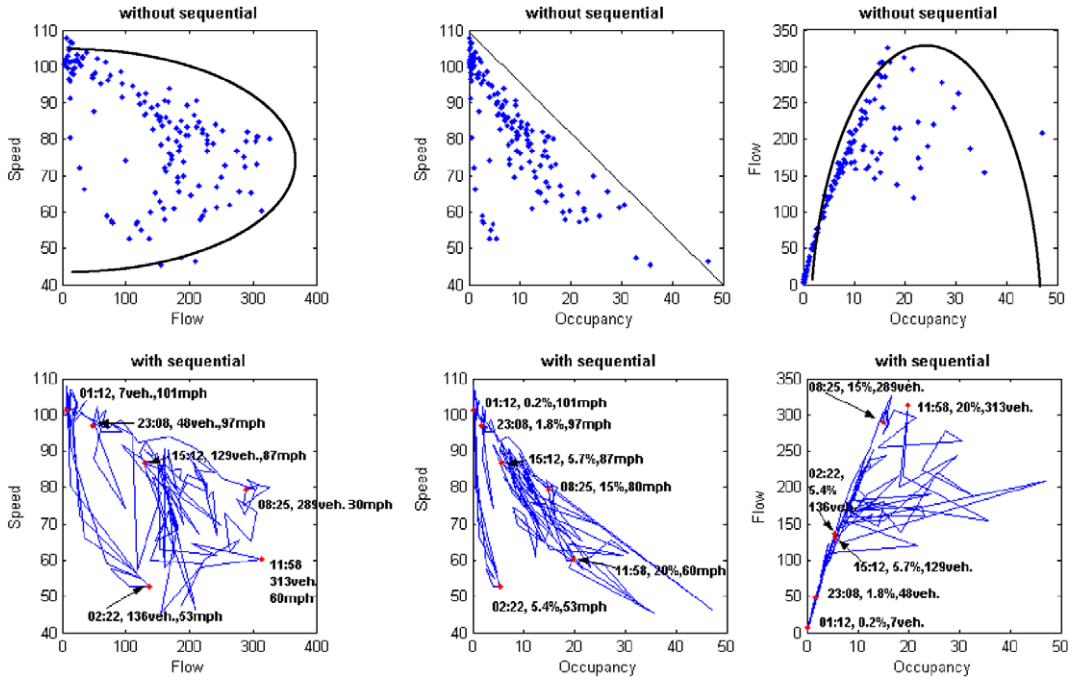

Fig. 10. The paired-traffic relationship and dynamics (station 421, 2004.02.04).

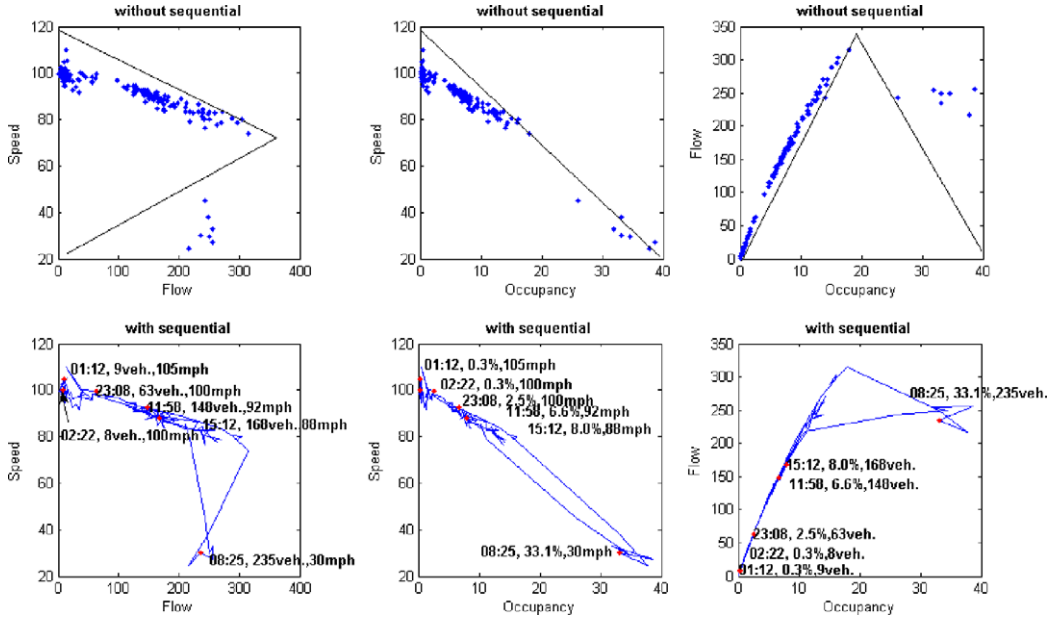

Fig. 11. The paired-traffic relationship and dynamics (station 433, 2004.02.04).

afternoon peak-hours the dynamics of speed-flow returns to the original upper left corner (free traffic phase); e.g., the fifth point at time 23:08 (48 vehicles/9-min, 97 kph).

In the light of the sequential order of speed-flow dynamics, we can see that congestion or near congestion can easily formulate as traffic switches from a high-speed, low-volume free-flow phase to an irregular moderate-speed, moderate-volume synchronized phase or the low-speed, low-volume congested phase. In reality, the transition occurs whenever the occupancy has exceeded a critical level. Once the traffic dynamics enters the congestion phase, it takes a long time for traffic to return to free-flow, and meanwhile delay accumulates. We also notice that from Fig. 10 there is a sixth point in the early hours at time 02:22 (136 vehicles/9-min, 53 kph) which indicates a relatively slow traffic flow, an outlier for free flow. It could have arisen from erratic driver behaviors, heterogeneous vehicle performances and any incident all the time. In contrast to Fig. 10, the paired-traffic in Fig. 11 seems to be quite fluent. From the locations at station 433 and station 421, one can definitely know that commuters regularly drive vehicles to work from their origin through station 433 to the destination (station 421) in the morning peak-hour. Such situations have caused congestion or near congestion traffic phase at station 421. Although a congestion traffic phase, i.e., high volume (235 vehicles/9-min), low speed (30 kph), high occupancy (33.1%) can also be seen at station 433 at rush hour, the congested traffic phase disappears after morning peak-hours. Compared with station 433, the congested traffic phase at station 421 does not disappear instantaneously but get worse because of the tremendous number of vehicles continuously coming from on-ramps. Hence, for seriously congested locations, such as station 421, had a rapid detection system successfully diagnosed the recurring congestions and a smart control measure actuated accordingly, the congestions have been immediately mitigated or alleviated.

In a similar way, three-variable traffic (flow–speed–occupancy) dynamics in three-dimensions is shown in Fig. 12. The trajectory moves from the coordinate (flow = 0, speed = 100, occupancy = 0), advances along a diagonal direction, i.e., coordinate (flow = 350, speed = 40, occupancy = 50) till morning peak-hours, when it moves back and forth as time evolves. Finally, similar to the one-day dynamics, the trajectory moves back to the original coordinate. In order to understand the progression in traffic dynamics, the purple lines in Fig. 12[5]

[5] For interpretation of the references to color in Fig. 12, the reader is referred to the web version of this article.

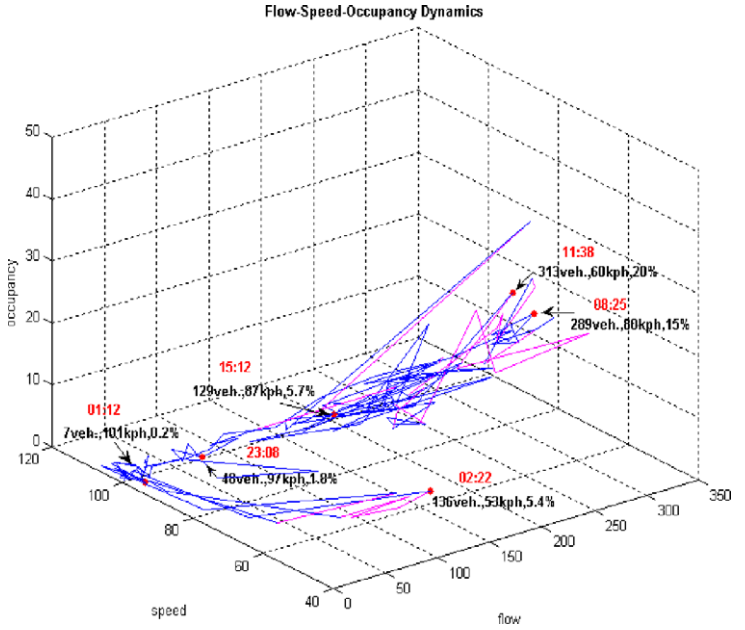

Fig. 12. The flow-speed-occupancy dynamics in three-dimensions.

represent those speeds less than 70 kph, and they appear intermittently among the blue lines which speed is over than 70 kph. It suggests that the quality of traffic flow progresses in a moderately dense platoon, in which traffic cannot move smoothly, but moves in a stop and go motion. If traffic data is collected from upstream ahead of a bottleneck, some trajectories of purple lines would probably not appear intermittently, but show together in some part of space. Obviously, from traffic control and management practice perspectives, depicting traffic characteristics with three variables simultaneously and with sequential order in three dimensional spaces is more subtle than just presenting any of these three variables in one-dimensional space.

Summarizing, the speed-flow dynamical graphs with sequential order can not only interpret the conventional speed-flow relationship but also present details of traffic phase-transition, which could provide more useful information for management and control purposes. Similarly, Figs. 10 and 11 have been used to compare graphical data for the dynamics without sequential order and with sequential order. From the above observations, we have learned that there are various traffic phases under normal circumstance: a free flow phase, which typically takes place in the early hours; a moving jam phase, which typically happens in the peak periods; and a synchronized traffic phase, a repeated back and forth transition, which more likely coexists with a moving jam.

6. Discussions

In this study, real world traffic variable (flow, speed, and occupancy) patterns extracted from isolated detecting stations have been characterized with varied trends and drastic fluctuations in reconstructed state spaces. Meanwhile, some traffic evolutions for paired- and three-variable were observed. After comparing the diverse features of traffic time series in reconstructed state spaces, we summarize some important findings and explain their nature here.

6.1. Temporal patterns

According to the parameters of successive one-month vs. one-day traffic time-series, the former state trajectories, which exhibit distinct time delay, unchangeable embedding dimension, near zero largest Lyapunov exponent and saturated correlation dimension, are characterized as having periodic-like patterns, which is as

anticipated. In contrast, the latter state trajectories of very short times (i.e., 20-s and 1-min) display random motions, and since their time delay is equal to one, embedding dimension is larger with increasing quantity of data, and correlation dimension is not saturated. Both state trajectories exhibit nonlinear dynamic features, one is the periodic-like dynamic and the other is the random dynamic. Following the above, we investigated a 10-workday traffic time-series at various times of day and inspected their parameters. The diversity of patterns which contain fixed point, deterministic-like patterns and stochastic patterns were explored. In other words, different nonlinear phenomena were found to emerge depending on the measured time scales, time-of-day and history data. However, the chaotic feature was not obtained in traffic time-series extracted from dual-loop detectors. Perhaps, further inspecting spatiotemporal features of congested traffic patterns can answer the question about chaotic or other complex behavior traffic characteristic.

We regard those traffic patterns attributed to deterministic-like dynamics as having some intrinsic rules governing the regularity. What do the real meanings or phenomena imply for such intrinsic rules in our daily life? We may assume that most trip makers get to work by 9 am and finish work at 5 pm on workdays, that is, they leave their homes or work places at approximately the same times, using the same modes, and/or choosing the same routes everyday. Such macroscopic regularities have caused ''similar but not exactly the same'' trends (i.e., slight fluctuations still exist) from day to day. Moreover, due to the constraints of travel demand, roadway capacity, speed limit, and so on, the observed traffic flows would not go beyond two extreme values: zero (free or jam) flow and maximum (capacity) flow. The speed and occupancy dynamics are also bounded within two extreme values (from free-flow speed or near zero occupancy to near zero speed or jammed occupancy). Thus, if we investigate the traffic time-series on successive days, many recurrent curves are expected to be exhibited in 1-D plot, and cyclic patterns would appear in 3-D spaces. The macroscopic regularities indeed dominate the shape (trend) of such deterministic-like traffic patterns.

However, it is noticed that not every driver is completely confined by such macroscopic regularities. The majority of drivers always control his/her vehicle at a desired speed and safe spacing and clearance so as to best interact with roadway environments and neighboring vehicles. The presence of human behavior is perhaps a key factor making traffic dynamics more complicated than many other physical systems that do not involve human behavior. Besides, roadway traffic is essentially composed of heterogeneous vehicles with diverse powers or maneuver capabilities. Hence, due to the heterogeneity across drivers and vehicles, the microscopic traffic dynamics will always fluctuate and surge along with the macroscopic traffic trend. Namely, the heterogeneity of drivers and vehicles not only elucidates the random feature of one-workday traffic series but also explains the phenomenon of ''similar but not exactly the same'' patterns for successive (many-workday) traffic series.

6.2. Spatiotemporal patterns

Although our research attempt only aimed at characterizing the evolutional trajectories of time-varying traffic features, we also probed the traffic phases between upstream and downstream stations in this paper. For example, we found congested traffic at station 421 in the morning peak-hour. According to three-phase traffic theory, congested traffic occurs most at freeway bottlenecks where can be a result of road-works, on- and off-ramps, a decrease in the number of freeway lanes, road curves and road gradients, etc. For an isolated bottleneck, there are two types of patterns in congested traffic: ''synchronized flow pattern (SP)'' and ''general pattern (GP).'' The GP is a congested pattern, which consists of synchronized flow upstream of an effectual bottleneck and wide moving jams that emerge spontaneously in that synchronized flow. For two or more adjacent bottlenecks, then an expanded congested pattern (EP) can be formed. In the EP, a synchronized flow phase or a complex interactive process among various moving jams could be anticipated. However, conventional theories, such as shock wave theory and queuing theories, and those models based on the fundamental diagram approach or a few results simulated by cellular automata (CA) models are hampered by lack of capability of predicting fundamental empirical features of phase transitions and spatiotemporal congested pattern features of real traffic. This is because spatiotemporal solutions of these models are in a fundamental qualitative contradiction with empirical (measured) traffic breakdown and the resulting congested patterns. Only the main spatiotemporal pattern features are fully understood, additional study of some nonlinear pattern features can be performed (Kerner, 2004).

By contrast, in the example of our paired-traffic features, speed and flow can transform from a free-flow phase in the early hours to a synchronized or congested phase in the morning peak-hours, during which the 9-min lane-flow rates can range from 7 vehicles to 289 vehicles and the corresponding time-mean-speed can drop from 101 kph to 80 kph. This suggests that an influx of vehicles in the morning peak-hour pushes the occupancy over a critical level, forcing the free-traffic phase into the moving jam or synchronized phase. The onset of traffic congestion is accompanied by a sharp drop in average vehicle speed, known as "the breakdown phenomenon". Even near noon, the flow rates remain high and the congested traffic does not disappear until around 14:00 pm. Unfortunately, the afternoon peak-hour arrives quickly thereafter thus the traffic state does not return to free-flow. Such irregular back-and-forth speed-flow features in the real world indicate that the synchronized traffic phase and the moving jams are alternative, which is similar to general pattern (GP). For such recurrent congestion, if a smart ramp metering instantaneously holds back the incoming vehicles in such a way that occupancy is kept below its critical value, traffic would flow freely and congestion could be avoided altogether. In sum, our observed paired- and three-variable traffic evolutions at the isolated detectors in effect provide evidence in support of Kerner's three-phase traffic theory and tackle the field problems.

7. Concluding remarks

In this paper, we have conceptualized the reconstruction of traffic series by creating appropriate embedding spaces to investigate the temporal traffic patterns. According to our empirical results, the proposed analytical method permits extracting more information on traffic series in reconstructed state spaces, particularly, unfolding the motions of flow, speed, and occupancy state trajectories, which could converge, diverge, or perform periodic motions. However, in contrast with temporal traffic patterns that occur only in time at specific locations, spatiotemporal traffic patterns that occur in both time and space can also be investigated. Different methodologies having certain advantages may achieve some purposes and thus we intend to further investigate more spatiotemporal patterns in future research.

In reality, it remains difficult to reproduce the reconstructed traffic time series by mathematical forms to serve as a dynamic traffic forecasting application in shorter time scales, such as 20-s and 1-min. Therefore, one challenge for further study is to develop logical basis for predictive models and control tactics by utilizing such processed traffic information from the reconstructed state spaces.

Acknowledgements

The authors are indebted to editor-in-chief for giving us chances to clarify and revise our original work. We are thankful to two anonymous reviewers for their constructive comments and suggestions to improve the quality of this paper. This study is part of the research projects granted by the ROC National Science Council (NSC-91-2211-E-009-048, NSC-92-2211-E-009-058 and NSC-95-2416-H-009-020-MY3).

References

Abarbanel, H.D.I., 1996. Analysis of Observed Chaotic Data. Springer-Verlag, New York.

Ansley, C.F., Spivey, W.A., Wrobleski, W.J., 1977. On the structure of moving average processes. Journal Econometrics 6, 121–134.

Box, G.E.P., Hillmer, S.C., Tiao, G.C., 1976. Analysis and modeling of seasonal time series. N.B.E.R. – Census Conference on Seasonal Time Series, Washington, DC.

Chang, J.L., Miaou, S.P., 1999. Real-time prediction of traffic flows using dynamic generalized linear models. Transportation Research Record 1678, 168–178.

Clarke, B.R., 1983. An algorithm for testing goodness of fit of ARMA (P, Q) models. Applied Statistics 32, 335–344.

Dendrinos, D.S., 1994. Traffic-flow dynamics: a search for chaos. Chaos, Solitons & Fractals 4, 605–617.

Disbro, J.E., Frame, M., 1989. Traffic flow theory and chaotic behavior. Transportation Research Record 1225, 109–115.

Fraser, A.M., Swinney, H.L., 1986. Independent coordinates for strange attractors from mutual information. Physical Review A 33, 1134–1140.

Grassberger, P., Procaccia, I., 1983. Measuring the strangeness of strange attractors. Physica D 9, 189–208.

Hilborn, R.C., 2000. Chaos and Nonlinear Dynamics: An Introduction for Scientists and Engineers, second ed. Oxford University Press, New York.

Jenkins, G.M., Alavi, A.S., 1981. Some aspects of modeling and forecasting multivariate time series. Journal of Time Series Analysis 2, 1–47.

Kants, H., Schreiber, T., 2004. Nonlinear Time Series Analysis. Cambridge University Press, Cambridge, UK.

Kennel, M.B., Brown, R., Abarbanel, H.D.I., 1992. Determining embedding dimension for phase-space reconstruction using a geometrical construction. Physical Review A 45, 3403–3411.

Kerner, B.S., 1998. A Theory of Congested Traffic Flow. In: Proceedings of the 3rd Symposium on Highway Capacity and Level of Service 2, pp. 621–642.

Kerner, B.S., 1999. Congested traffic flow: observations and theory. Transportation Research Record 1678, 160–167.

Kerner, B.S., 2002a. Synchronized flow as a new traffic phase and related problems for traffic flow modeling. Mathematical and Computer Modeling 35, 481–508.

Kerner, B.S., 2002b. Empirical macroscopic features of spatial–temporal traffic patterns at highway bottlenecks. Physical Review E 65, 046138.

Kerner, B.S., 2004. The Physics of Traffic. Springer, Berlin, New York.

Kerner, B.S., Klenov, S.L., 2002. A microscopic model for phase transitions in traffic flow. Journal of Physics A: Mathematical and General 35, L31–L43.

Kerner, B.S., Klenov, S.L., Wolf, D.E., 2002. A cellular automata approach to three-phase traffic theory. Journal of Physics A: Mathematical and General 35, 9971–10013.

Kerner, B.S., Rehborn, H., Aleksic, M., Haug, A., 2004. Recognition and tracking of spatial–temporal congested traffic patterns on freeways. Transportation Research Part C 12, 369–400.

Kerner, B.S., Klenov, S.L., Hiller, A., 2006. Criterion for traffic phase in single vehicle data and empirical text of three-phase traffic theory. Journal of Physics A: Mathematical and General 39, 2001–2020.

Lan, L.W., Lin, F.Y., Kuo, A.Y., 2003. Testing and prediction of traffic flow dynamics with chaos. Journal of the Eastern Asia Society for Transportation Studies 5, 1975–1990.

Lee, S., Fambro, D.B., 1999. Application of subset autoregressive integrated moving average model for short-term freeway traffic volume forecasting. Transportation Research Record 1678, 179–188.

Lingras, P., Sharma, S.C., Osborne, P., 2000. Traffic volume time-series analysis according to the type of road use. Computer-Aided Civil and Infrastructure Engineering 15, 365–373.

Liu, L.M., Lin, M.W., 1991. Forecasting residential consumption of natural gas using monthly and quarterly time series. International Journal of Forecasting 7, 3–16.

Maravall, A., 1983. An application of nonlinear time series forecasting. Journal Business Economic Statistics 1, 66–74.

May, A.D., 1990. Traffic Flow Fundamentals. Prentice Hall, New Jersey.

Nayfeh, A.H., Balachandran, B., 1995. Applied Nonlinear Dynamics. John Wiley & Sons, Inc., New York.

Shang, P., Li, X., Kamae, S., 2005. Chaotic analysis of traffic time series. Chaos, Solitons & Fractal 25, 121–128.

Sheu, J.B., Chou, Y.H., Chen, A., 2004. Stochastic modeling and real-time prediction of incident effects on surface street traffic congestion. Applied Mathematical Modelling 28, 445–468.

Smith, B.L., Williams, B.M., Oswald, R.K., 2002. Comparison of parametric and nonparametric models for traffic flow forecasting. Transportation Research Part C 10, 303–321.

Stathopoulos, A., Karlaftis, M.G., 2003. A multivariate state space approach for urban traffic flow modeling and prediction. Transportation Research Part C 11, 121–135.

Takens, F., 1981. Detecting strange attractors in turbulence. Dynamical systems and turbulence. In: Lecture Notes in Mathematics, vol. 898. Springer, New York.

Varaiya, P., 2005. What we've learned about highway congestion. Access 27, 2–9.

Williams, B.M., 2001. Multivariate vehicular traffic flow prediction: an evaluation of ARIMAX modeling. In: Transportation Research Board Annual Meeting, Washington, DC, pp. 194–200.

Williams, B.M., Hoel, L.A., 2003. Modeling and forecasting vehicular traffic flow as a seasonal ARIMA process: theoretical basis and empirical results. Journal of Transportation Engineering 129, 664–672.

Zhang, X., Jarrett, D.F., 1998. Chaos in a dynamic model of traffic flows in an origin–destination network. Chaos 8, 503–513.